B_{1g}-Phonon Anomaly Driven by Fermi Surface Instability at Intermediate Temperature in $YBa_2Cu_3O_{7-\delta}$

Dongjin Oh,[1,2] Dongjoon Song,[1,2] Younsik Kim,[1,2] Shigeki Miyasaka,[3] Setsuko Tajima,[3] Jin Mo Bok,[4,5] Yunkyu Bang,[4,5] Seung Ryong Park,[6,7,*] and Changyoung Kim[1,2,†]

[1]*Center for Correlated Electron Systems, Institute for Basic Science, Seoul 08826, Korea*
[2]*Department of Physics and Astronomy, Seoul National University, Seoul 08826, Korea*
[3]*Department of Physics, Osaka University, Osaka 560-0043, Japan*
[4]*Department of Physics, Pohang University of Science and Technology, Pohang 37673, Republic of Korea*
[5]*Asia Pacific Center for Theoretical Physics, Pohang 37673, Korea*
[6]*Department of Physics, Incheon National University, Incheon 22012, Republic of Korea*
[7]*Intelligent Sensor Convergence Research Center (ISCRC), Incheon National University, Incheon 22012, Republic of Korea*

(Received 2 July 2021; revised 14 October 2021; accepted 6 December 2021; published 29 December 2021)

We performed temperature- and doping-dependent high-resolution Raman spectroscopy experiments on $YBa_2Cu_3O_{7-\delta}$ to study B_{1g} phonons. The temperature dependence of the real part of the phonon self-energy shows a distinct kink at $T = T_{B1g}$ above T_c due to softening, in addition to the one due to the onset of the superconductivity. T_{B1g} is clearly different from the pseudogap temperature with a maximum in the underdoped region and resembles charge density wave onset temperature, T_{CDW}. We attribute the B_{1g}-phonon softening to an energy gap on the Fermi surface induced by a charge density wave order, which is consistent with the results of a recent electronic Raman scattering study. Our work demonstrates a way to investigate Fermi surface instabilities above T_c via phonon Raman studies.

DOI: 10.1103/PhysRevLett.127.277001

In strongly correlated electron systems, instabilities with complex order parameters are often accompanied by electronic orders that cause various broken symmetries and Fermi surface instabilities in the ground state. The instabilities generically lead to an energy gap at the Fermi surface to lower the energy of the system. The most representative cases are the Cooper pair and Peierls instabilities that are associated with superconductivity and charge density wave (CDW), respectively. In the former case, the superconducting ground state is created through the coherent superposition of electrons, and the superconducting gap is opened in the presence of weak attractive interaction between electrons. Similarly in the latter case, coherent electron-hole pairs create a CDW gap [1,2].

The gap opening driven by an electronic instability affects not only the electronic but also phononic excitation spectra. For example, it is well known that the B_{1g} oxygen bond-buckling phonon in copper oxide high-T_c superconductors shows a softening when the temperature is lowered below T_c [3–6]. The origin of the phonon anomaly was understood to be from a phonon self-energy effect caused by the opening of the superconducting gap 2Δ (see Fig. 1); the phonon peak in the Raman spectrum exhibits narrowing due to the reduced scattering rate upon gap opening. In contrast, phonons with $\omega > 2\Delta$ show broadening since, for such phonons, scattering channels are available and their scattering rate increases due to the increased quasiparticle density of states (DOS). In this way, we can indirectly infer the existence of a superconducting gap. In addition to the superconductivity, this explanation can be also applied to other electronic orders such as CDW which gives rise to an energy gap [7].

Among the various phonon modes in copper oxide superconductors, only the B_{1g} phonon shows a noticeable renormalization in the Raman spectra as we mentioned above. This result drew much interest since it may reflect the intimate link between superconductivity and B_{1g} phonon. Indeed, the coupling constant between electrons and B_{1g} phonon at the Brillouin zone center ($q = 0$) possesses a d-wave nature, which is the symmetry of the superconductivity as well as CDW form factor in cuprates [8–12]. Such character allows the B_{1g} phonon to strongly couple with the electrons near the antinode where the superconducting gap is the maximum. As a result, a strong renormalization in the electronic structure appears in the form of a kink or peak-dip-hump feature near the anti-nodal region [13,14]. A recent theoretical work pointed out that the B_{1g} phonon may induce a charge order in underdoped copper oxide superconductors [15,16].

A possible way to address the issues described above is to investigate how the electronic structure in various phases of copper oxide superconductors affects the B_{1g}-phonon mode. In this Letter, we present results of comprehensive doping- and temperature-dependent high-resolution Raman

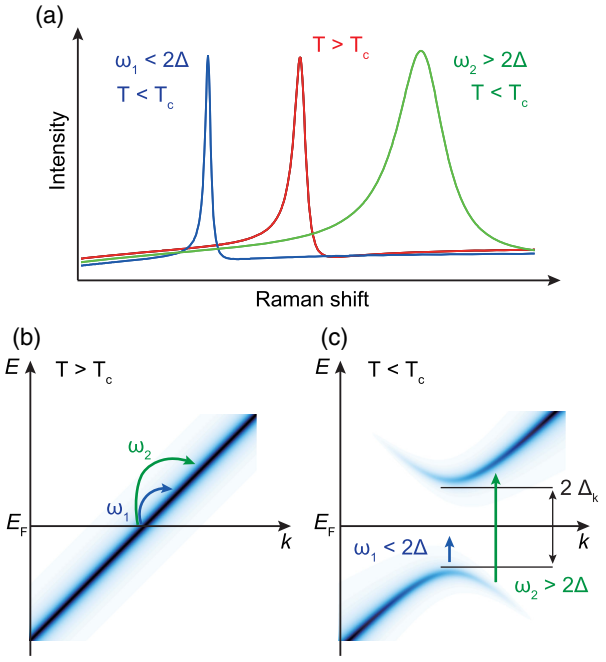

FIG. 1. (a) Sketch of the phonon renormalization due to the phonon self-energy effect. The red curve represents a phononic Raman spectrum in the normal state. Blue and green curves correspond to the spectrum in the ordered state for the phonon energy $\omega < 2\Delta$ and $\omega > 2\Delta$, respectively. Schematic of the low energy electronic structure of a superconductor (b) above and (c) below the critical temperature, T_c.

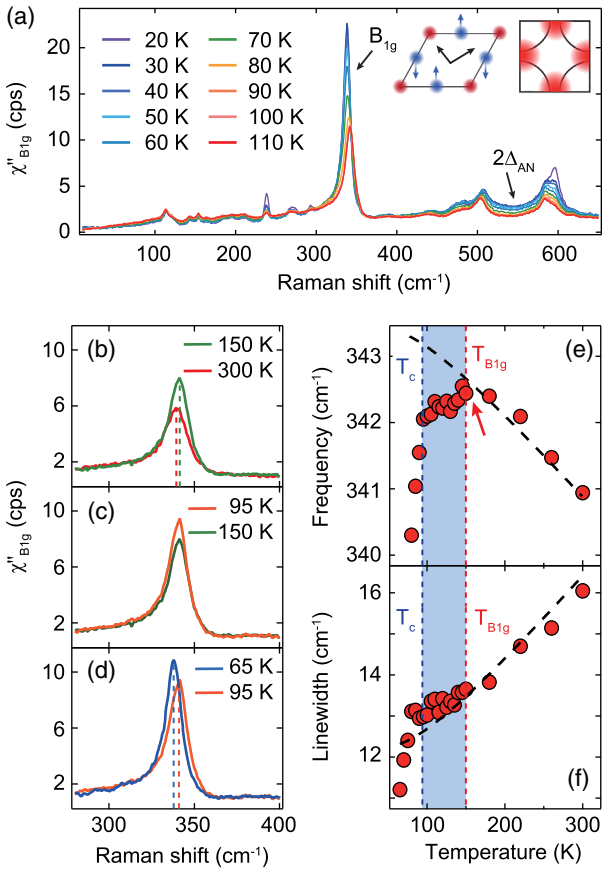

FIG. 2. (a) Temperature-dependent Raman response of optimally doped $YBa_2Cu_3O_{7-\delta}$ (OP94) single crystal below 110 K. The peak at 340 cm^{-1} corresponds to the B_{1g} phonon and the broad peak around 550 cm^{-1} is due to pair breaking peak. The left inset is the schematic for the B_{1g} phonon seen from the perspective view. Compared are B_{1g}-phonon spectra measured at (b) 300 and 150 K, (c) 150 and 95 K, and (d) 95 and 65 K. Temperature-dependent frequency (e) and linewidth (f) extracted from a Fano lineshape fitting. The black dashed curve corresponds to simulated frequency and linewidth of the B_{1g} phonon from the phonon anharmonicity model. The blue and red vertical dashed lines represent the superconducting transition temperature (T_c) and onset temperature of the phonon anomaly (T_{B1g}), respectively.

spectroscopy studies on $YBa_2Cu_3O_{7-\delta}$. Owing to the very high-statistics data, our results clearly show that phonon softening occurs not only in the superconducting state but also at a temperature higher than T_c which has not yet been reported. The softening is robust in the underdoped region but is not observed for the most overdoped sample. The onset temperature of the phonon anomaly, T_{B1g}, is distinguished from the pseudogap temperature T^*. It is rather close to the CDW temperature, T_{CDW}. Our experimental results can be interpreted that the Fermi surface instability induced by the charge density wave order causes the softening of the B_{1g} phonon. Our results can serve as experimental evidence for the existence of a CDW gap in the copper oxide superconductors.

We performed Raman spectroscopy with backscattering geometry using 532 nm (2.3 eV) diode pumped solid-state (DPSS) laser (Cobolt). The incident light was focused on the surface of the sample by a ×40 (N.A. 0.6) objective lens (Olympus). The spot size of the focused light was approximately 2×2 μm^2 and laser power was set below 0.6 mW to avoid laser-induced local heating. To reject the stray light close to 10 cm^{-1}, BragGrate notch filters (OptiGrate) were used. The superachromatic wave plate (Thorlabs) was used for polarization-resolved Raman spectroscopy. The polarization of the incident and scattered light was set to be perpendicular to each other and parallel to the diagonal direction of the CuO_2 plaquette [Fig. 2(a), inset] to probe the signal from the B_{1g} channel. The direction of the Cu−O bonding was determined by the angle-resolved polarized Raman scattering measurement (see Sec. I of the Supplemental Material) [17]. The Raman scattered light was collected by the same objective lens and collimated before entering the focusing lens in front of the spectrometer. The collected light was dispersed by a Jobin-Yvon Horiba iHR320 spectrometer with 1800 grooves/mm grating and detected by a thermoelectric cooled CCD. Twinned $YBa_2Cu_3O_{7-\delta}$ single crystals were mounted on an optical cryostat (Oxford) for temperature-dependent measurements. Optimally doped $YBa_2Cu_3O_{7-\delta}$ single crystals were annealed in a tube furnace with oxygen flow

to control the oxygen content. The superconducting transition temperature was determined from the diamagnetic signal measured with a magnetic property measurement system (Quantum Design) (see Sec. II of the Supplemental Material) [17]. The typical size of the crystals is $2 \times 2 \times 0.5$ mm^3. The measured Raman spectra were divided by Bose-Einstein factor to present Raman susceptibility χ''.

We first briefly touch upon how the gap in the electronic phase can affect the phonon peaks in Raman spectra. Plotted in Fig. 1 is a schematic of the low energy single particle spectral function across the superconducting gap and its effect on a phonon peak in Raman spectra. In the superconducting state, the superconducting gap opens at the Fermi surface while quasiparticle DOS at $\omega = \pm\Delta$ is enhanced. It results in a singularity at $\omega = 2\Delta$ in the real and imaginary parts of the phonon self-energy [22,23]. At $T < T_c$, for a phonon with ω_{ph} smaller (larger) than 2Δ, softening (hardening) and narrowing (broadening) of the phonon is expected, in comparison to the $T > T_c$ case [Fig. 1(a)]. This phenomenon can be intuitively understood as follows. In the normal state, all phonons can be scattered by coupling to the electrons near the Fermi level [Fig. 1(b)]. In the superconducting state, however, phonons with $\omega_{\mathrm{ph}} < 2\Delta$ cannot be scattered by electrons due to the lack of scattering channels. On the other hand, the scattering rate of $\omega_{\mathrm{ph}} > 2\Delta$ phonons increases due to the enhanced quasiparticle DOS [Fig. 1(c)].

Figure 2(a) shows the B_{1g} Raman response of optimally doped ($T_c = 94$ K) $YBa_2Cu_3O_{7-\delta}$. As the temperature decreases below T_c, a broad electronic Raman continuum appears near 550 cm^{-1}. It is a signature of superconducting pair breaking peak, $2\Delta_{\mathrm{AN}}$, representing the superconducting gap near the antinodal region in the Brillouin zone [Fig. 2(a), inset] [24,25]. The strongest peak at 340 cm^{-1} corresponds to the B_{1g} phonon. Consistent with previous results, our results also show hardening in the normal state [Fig. 2(b)] and strong softening below T_c [Fig. 2(d)] [3–6]. However, an additional weak phonon softening was observed for a temperature range just above T_c [Fig. 2(c)]. To quantify the phonon softening, we extracted the frequency and line width of the B_{1g} phonon by fitting the peak with a Fano line shape [3,6,26]. Figures 2(e) and 2(f) show the frequency and linewidth of the B_{1g} phonon, respectively, as a function of temperature. The black dashed curves represent the simulated frequency and linewidth behavior using a phonon anharmonicity model [27]. Above 150 K, phonon hardening was well described by the phonon anharmonicity. The frequency of the B_{1g} phonon begins to deviate from the anharmonic behavior around 150 K. The frequency decreases slowly until the temperature reaches T_c, then decreases rapidly below T_c. In Fig. 2(f), the linewidth of the B_{1g} phonon also appears to deviate from the black dashed curve above T_c. However, if higher order terms are added to the phonon anharmonicity model, the linewidth data can be fitted well from T_c to 300 K (see Sec. IV of the Supplemental Material) [17]. Hence, we define the onset temperature of the phonon anomaly, dubbed as T_{B1g}, from the temperature versus frequency data.

To verify the doping dependence of T_{B1g}, we performed the same experiment and analysis on samples with various dopings. We find that not only the optimally doped sample but also underdoped samples (UD62, UD68, and UD85) [Figs. 3(a)–3(c), respectively] clearly show the B_{1g}-phonon anomaly between T_c and T_{B1g}. On the other hand, the phonon anomaly significantly weakens for a slightly overdoped sample [Fig. 3(d)] and vanishes for the most overdoped sample [Fig. 3(e)]. This indicates the fact that the instability that causes the B_{1g}-phonon anomaly disappears in the overdoped region. An interesting observation is that the magnitude of B_{1g}-phonon softening is proportional to the T_c (T_{B1g}) in the superconducting (normal) phase (refer to Sec. VI of the Supplemental Material for more details) [17].

Plotted in Fig. 4 are the measured T_{B1g} (filled red circles) with the onset temperatures of various phases. The value of

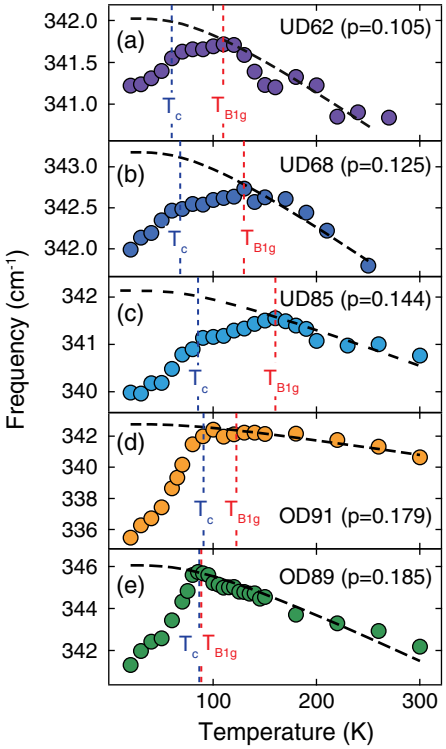

FIG. 3. Temperature-dependent B_{1g}-phonon frequency from $YBa_2Cu_3O_{7-\delta}$ single crystals with different dopings. Results for UD62 (a), UD68 (b), UD85 (c), OD91 (d), OD89 (e). The hole doping concentration was determined using the method in Ref. [28]. T_c and T_{B1g} are indicated by blue and red vertical dashed lines, respectively.

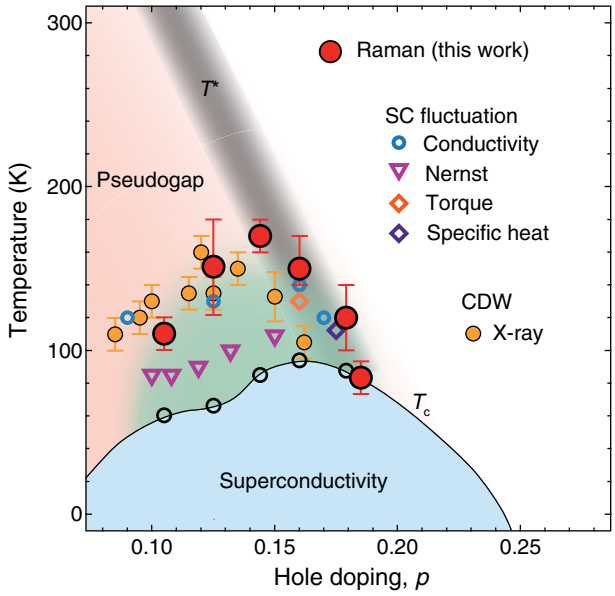

FIG. 4. $YBa_2Cu_3O_{7-\delta}$ phase diagram with various phases determined by various techniques. T_{B1g} extracted from our Raman spectroscopy data is plotted as red circles. Superconducting fluctuation temperature (T_{pair}) in $YBa_2Cu_3O_{7-\delta}$ measured by various methods are also plotted: magnetoconductivity (blue circles) [29], Nernst (violet inverted triangles) [30], torque magnetometry (orange diamonds) [31], and specific heat (purple diamonds) [32]. T_{CDW} measured by resonant x-ray scattering (RXS) [33] is plotted as yellow circles. Black shaded line represents the T^* that can be found elsewhere [21,34].

T_{B1g} is highest near slightly underdoping ($p = 0.144$) and decreases as the hole doping concentration increases or decreases. It is clearly seen that the doping dependence of T_{B1g} is quite different from that of T^* because T^* monotonously increases as the hole doping concentration decreases. This strongly suggests that the B_{1g}-phonon anomaly is not caused by the pseudogap. Instead, T_{B1g} appears to be closer to T_{CDW}.

From the point of view that T_{B1g} corresponds to T_{CDW}, the phonon softening above T_c can be attributed to the formation of a CDW order. Although T_{B1g} does not match previously reported T_{CDW} very well, there is a reasonable similarity between T_{CDW} and T_{B1g} since the overall doping dependence of these temperature scales shows a very similar trend. Then, an immediate culprit for the observed phonon softening is the Kohn anomaly through which phonons are softened in the CDW phase [1,35]. In this case, a giant phonon anomaly can occur at $q = q_{CDW}$. However, B_{1g}-phonon softening in our results cannot be reconciled with the Kohn anomaly since the first-order Raman scattering probes $q \sim 0$ phonons.

It is more natural to interpret that phonon softening at $q \sim 0$ comes from the phonon self-energy effect due to the Fermi surface reconstruction induced by CDW [7] (see Sec. VII of the Supplemental Material) [17]. Indeed, the energy scale of the CDW gap (> 600 cm^{-1}) measured by the electronic Raman scattering experiment is much larger than that of the B_{1g} phonon (340 cm^{-1}) [21]. In this case, the B_{1g} phonon can be softened as described above (Fig. 1). Based on these considerations, the mismatch between T_{CDW} and T_{B1g} can be understood as follows. Although no CDW peak was observed in resonant x-ray scattering (RXS) studies, inelastic neutron scattering results showed the softening of B_{1g} phonon at $q = q_{CDW}$ even for the most overdoped $YBa_2Ca_3O_7$ [7,33]. It suggests the existence of CDW fluctuation even for the doping range where no static CDW order is observed. If the dynamic CDW affects the phonon self-energy, T_{B1g} may exhibit a different temperature scale than that measured by RXS. This calls for further studies with various experimental tools in the doping range where CDW order exists.

Although softening of the B_{1g} phonon can be explained by the emergence of a CDW gap, we may not entirely rule out the possibility that superconducting fluctuation causes the phonon softening in the intermediate temperature range. Except for T_{pair} obtained from a Nernst effect study [30], the temperature scales of the superconducting fluctuation from magnetoconductivity [29], torque magnetometry [31], and specific heat [32] are quite close to our T_{B1g}. In this temperature range, preformed Cooper pairs can open a gap at the Fermi surface and enhance the quasiparticle DOS at $\omega = \pm\Delta$, which has been clearly observed in a recent angle-resolved photoemission spectroscopy (ARPES) study on Bi2212 [36]. However, the pair breaking peak in the B_{1g} electronic Raman spectra, which indicates the formation of superconducting gap, was not observed in the temperature range between T_c and T_{B1g} (see Sec. VIII of the Supplemental Material) [17]. Considering our electronic Raman results, it should be more natural to understand that the anomalous B_{1g}-phonon softening above T_c observed in our experiments caused by a CDW gap in the intermediate temperature range.

While our results demonstrated definite coupling between B_{1g} phonon and the possible CDW phase in the intermediate temperature range, they may not provide direct evidence for an active role of the B_{1g} phonon in the formation of the CDW or other phases as has been argued previously [15,16]. To investigate the active role of the B_{1g} phonon for various electronic orders in copper oxide superconductors, systematic doping- and temperature-dependent studies on the B_{1g} phonon around phase boundary via diverse experiments are required. For example, pump-probe spectroscopic techniques that can perform a "coherent electron-phonon lock-in" measurement [37,38] on B_{1g} phonons may be a way.

We acknowledge the fruitful discussion with S. Jung and D. Wulferding. This work was supported by the Institute for Basic Science in Korea (Grant No. IBS-R009-G2). S. R. P. acknowledges support from the NRF (Grant

No. 2020R1A2C1011439). We also acknowledge support from the NRF (Grants No. NRF-2019R1I1A1A01057393, No. NRF-2020-R1A2C2-007930). Sample preparation was supported by the Grant-in-Aid for Scientific Research from the Ministry of Education, Culture, Sports, Science and Technology of Japan (Grants No. 19204038 and No. 24340083).

*AbePark@inu.ac.kr
†changyoung@snu.ac.kr

[1] G. Gruner, *Density Waves in Solids* (CRC Press, Boca Raton, 2018).
[2] J. Li and R. Comin, Nat. Phys. **15**, 736 (2019).
[3] E. Altendorf, X. K. Chen, J. C. Irwin, R. Liang, and W. N. Hardy, Phys. Rev. B **47**, 8140 (1993).
[4] M. F. Limonov, A. I. Rykov, S. Tajima, and A. Yamanaka, Phys. Rev. B **61**, 12412 (2000).
[5] K. C. Hewitt, X. K. Chen, C. Roch, J. Chrzanowski, J. C. Irwin, E. H. Altendorf, R. Liang, D. Bonn, and W. N. Hardy, Phys. Rev. B **69**, 064514 (2004).
[6] M. Bakr, A. P. Schnyder, L. Klam, D. Manske, C. T. Lin, B. Keimer, M. Cardona, and C. Ulrich, Phys. Rev. B **80**, 064505 (2009).
[7] M. Raichle, D. Reznik, D. Lamago, R. Heid, Y. Li, M. Bakr, C. Ulrich, V. Hinkov, K. Hradil, C. T. Lin, and B. Keimer, Phys. Rev. Lett. **107**, 177004 (2011).
[8] T. P. Devereaux, A. Virosztek, and A. Zawadowski, Phys. Rev. B **51**, 505 (1995).
[9] M. Opel, R. Hackl, T. P. Devereaux, A. Virosztek, A. Zawadowski, A. Erb, E. Walker, H. Berger, and L. Forró, Phys. Rev. B **60**, 9836 (1999).
[10] K. Fujita, M. H. Hamidian, S. D. Edkins, C. K. Kim, Y. Kohsaka, M. Azuma, M. Takano, H. Takagi, H. Eisaki, S.-I. Uchida *et al.*, Proc. Natl. Acad. Sci. U.S.A. **111**, E3026 (2014).
[11] R. Comin, R. Sutarto, F. He, E. H. da Silva Neto, L. Chauviere, A. Frano, R. Liang, W. N. Hardy, D. A. Bonn, Y. Yoshida *et al.*, Nat. Mater. **14**, 796 (2015).
[12] M. H. Hamidian, S. D. Edkins, C. K. Kim, J. C. Davis, A. P. Mackenzie, H. Eisaki, S. Uchida, M. J. Lawler, E.-A. Kim, S. Sachdev *et al.*, Nat. Phys. **12**, 150 (2016).
[13] T. P. Devereaux, T. Cuk, Z.-X. Shen, and N. Nagaosa, Phys. Rev. Lett. **93**, 117004 (2004).
[14] T. Cuk, F. Baumberger, D. H. Lu, N. Ingle, X. J. Zhou, H. Eisaki, N. Kaneko, Z. Hussain, T. P. Devereaux, N. Nagaosa, and Z.-X. Shen, Phys. Rev. Lett. **93**, 117003 (2004).
[15] S. Banerjee, W. Atkinson, and A. P. Kampf, Commun. Phys. **3**, 161 (2020).
[16] S. Banerjee, W. A. Atkinson, and A. P. Kampf, Phys. Rev. B **103**, 235141 (2021).
[17] See Supplemental Material http://link.aps.org/supplemental/10.1103/PhysRevLett.127.277001 for additional information on (I) experimental geometry and angle-resolved polarization dependent Raman spectra, (II) magnetization measurement, (III) electronic Raman spectra from B_{1g} channel, (IV) anharmonicity fitting with the higher-order terms, (V) doping- and temperature-dependent linewidth and asymmetric parameter q of B_{1g} phonon, (VI) numerical calculation of charge susceptibility with CDW ordering, and (VIII) temperature-dependent intensity of pair breaking peak in optimally doped $YBa_2Cu_3O_{7-\delta}$. The Supplemental Material includes Refs. [3,15,18–22].
[18] A. Sacuto, Y. Gallais, M. Cazayous, M.-A. Measson, G. D. Gu, and D. Colson, Rep. Prog. Phys. **76**, 022502 (2013).
[19] Z. Zhao, J. Elwood, and M. A. Carpenter, J. Phys. Chem. C **119**, 23094 (2015).
[20] D. L. Feng, D. H. Lu, K. M. Shen, C. Kim, H. Eisaki, A. Damascelli, R. Yoshizaki, J.-i. Shimoyama, K. Kishio, G. D. Gu *et al.*, Science **289**, 277 (2000).
[21] B. Loret, N. Auvray, Y. Gallais, M. Cazayous, A. Forget, D. Colson, M.-H. Julien, I. Paul, M. Civelli, and A. Sacuto, Nat. Phys. **15**, 771 (2019).
[22] R. Zeyher and G. Zwicknagl, Z. Phys. B **78**, 175 (1990).
[23] E. J. Nicol, C. Jiang, and J. P. Carbotte, Phys. Rev. B **47**, 8131 (1993).
[24] T. P. Devereaux and R. Hackl, Rev. Mod. Phys. **79**, 175 (2007).
[25] T. P. Devereaux, D. Einzel, B. Stadlober, R. Hackl, D. H. Leach, and J. J. Neumeier, Phys. Rev. Lett. **72**, 396 (1994).
[26] N. Driza, S. Blanco-Canosa, M. Bakr, S. Soltan, M. Khalid, L. Mustafa, K. Kawashima, G. Christiani, H.-U. Habermeier, G. Khaliullin *et al.*, Nat. Mater. **11**, 675 (2012).
[27] M. Balkanski, R. F. Wallis, and E. Haro, Phys. Rev. B **28**, 1928 (1983).
[28] R. Liang, D. A. Bonn, and W. N. Hardy, Phys. Rev. B **73**, 180505(R) (2006).
[29] F. Rullier-Albenque, H. Alloul, and G. Rikken, Phys. Rev. B **84**, 014522 (2011).
[30] O. Cyr-Choinière, R. Daou, F. Laliberté, C. Collignon, S. Badoux, D. LeBoeuf, J. Chang, B. J. Ramshaw, D. A. Bonn, W. N. Hardy, R. Liang, J.-Q. Yan, J.-G. Cheng, J.-S. Zhou, J. B. Goodenough, S. Pyon, T. Takayama, H. Takagi, N. Doiron-Leyraud, and L. Taillefer, Phys. Rev. B **97**, 064502 (2018).
[31] L. Li, Y. Wang, S. Komiya, S. Ono, Y. Ando, G. D. Gu, and N. P. Ong, Phys. Rev. B **81**, 054510 (2010).
[32] J. L. Tallon, J. G. Storey, and J. W. Loram, Phys. Rev. B **83**, 092502 (2011).
[33] S. Blanco-Canosa, A. Frano, E. Schierle, J. Porras, T. Loew, M. Minola, M. Bluschke, E. Weschke, B. Keimer, and M. Le Tacon, Phys. Rev. B **90**, 054513 (2014).
[34] L. Zhao, C. A. Belvin, R. Liang, D. A. Bonn, W. N. Hardy, N. P. Armitage, and D. Hsieh, Nat. Phys. **13**, 250 (2017).
[35] M. Le Tacon, A. Bosak, S. Souliou, G. Dellea, T. Loew, R. Heid, K. Bohnen, G. Ghiringhelli, M. Krisch, and B. Keimer, Nat. Phys. **10**, 52 (2014).
[36] S.-D. Chen, M. Hashimoto, Y. He, D. Song, K.-J. Xu, J.-F. He, T. P. Devereaux, H. Eisaki, D.-H. Lu, J. Zaanen *et al.*, Science **366**, 1099 (2019).
[37] S. Gerber, S.-L. Yang, D. Zhu, H. Soifer, J. A. Sobota, S. Rebec, J. J. Lee, T. Jia, B. Moritz, C. Jia *et al.*, Science **357**, 71 (2017).
[38] S.-L. Yang, J. A. Sobota, Y. He, D. Leuenberger, H. Soifer, H. Eisaki, P. S. Kirchmann, and Z.-X. Shen, Phys. Rev. Lett. **122**, 176403 (2019).